2019

Process planning for iterative, in-envelope hybrid manufacturing in the presence of machining allowances

Jakob Croghan
Iowa State University

Process planning for iterative, in-envelope hybrid manufacturing in the presence of machining allowances

by

Jakob Croghan

A thesis submitted to the graduate faculty

in partial fulfillment of the requirements for the degree of

MASTER OF SCIENCE

Major: Industrial Engineering

Program of Study Committee:
Matthew C. Frank, Major Professor
Peter Collins
Frank Peters

The student author, whose presentation of the scholarship herein was approved by the program of study committee, is solely responsible for the content of this thesis. The Graduate College will ensure this thesis is globally accessible and will not permit alterations after a degree is conferred.

Iowa State University

Ames, Iowa

2019

TABLE OF CONTENTS

LIST OF FIGURES

Page

LIST OF TABLES

Page

ABSTRACT

The objective of this research is to develop a method for an iterative hybrid manufacturing (HM) process to create straight wall geometries in the presence of tool reach and access limitations. The method specifically addresses the management of machining allowance added during deposition – required to be machined away, but also used to support subsequent deposition operations. This research will present the implementation of this method with an HM system utilizing directed energy deposition (DED) in combination with computer numerical control (CNC) machining.

Today's manufacturing environment is rapidly adopting hybrid manufacturing technologies, particularly those with the capability of producing end component geometry through both additive manufacturing (AM) and subtractive manufacturing processes. However, much of the use of these unique technologies is done in isolation, first producing a component's entire geometry via an AM process, and subsequently following with a subtractive process to produce the final surface geometry. This sequential approach fails to take advantage of the integrated nature of hybrid manufacturing, which allows changing between the two processes without adjusting fixturing. This is largely due to the complexity of these process changes and the implications removing material may have on the next application of AM methods. Utilizing a method that iteratively deposits material and then machines that deposition provides the ability to create unique and previously unattainable geometries. The proposed method will reduce the issues associated with material removal before a DED-AM process.

CHAPTER 1. INTRODUCTION

1.1 Background

Driven by cost pressures, increasingly prevalent sustainability initiatives, and a desire to produce increasingly complex designs, more manufacturing firms are adopting hybrid manufacturing (HM) systems. These systems combine an additive manufacturing (AM) process with another process to create final component geometry. An example of such a system is the combination of directed energy deposition (DED) with computer numerical control (CNC) machining. DED, a metal AM process, enables users to selectively deposit material onto a component. Due to the limitations of the process accuracy, DED is often used in combination with CNC machining to achieve desired specifications, particularly with regards to surface finish and dimensional tolerancing. The combination of DED and CNC machining in a hybrid manufacturing system has a wide variety of applications, ranging from component repair to end component creation. Multiple variants of DED have evolved utilizing different heat sources and feedstock options.

Hybrid manufacturing systems are not without their limitations. For example, applications with blown-powder DED processes have been fairly limited in their ability to create "tall" components due to CNC machine tooling limitations, particularly when it comes to tool reach and accessibility. Through the careful management of tool reach and access, including the use of additional machining axes, tall components have been produced using blown powder. A great deal of specialized knowledge regarding machine tooling and tool path planning is required to accomplish such a process. Due to the need to carefully consider part orientation, collision conditions, and the ability of tooling to reach the surface, tool path planning is often time intensive. This is complicated further as more axes are added, moving

from three-axis toolpaths to four- or five-axis toolpaths, requiring more specialized knowledge. This limitation of blown-powder DED systems is less severe when using a continuous wire-fed DED process. Due to the solid nature of the feedstock material, deposition can occur with minimal support structures and in a wider variety of angles or positions compared to blown-powder DED systems. This helps to simplify process planning in wire fed systems, but the approaches cannot be readily applied to other HM processes.

The goal of this research is to take the first steps to generate an automatic process planning method for HM systems involving the combination of AM with CNC machining. This method will allow for the management of machining allowances to not only achieve final part tolerances but also support subsequent AM depositions in a 3-axis configuration. This will be done by developing a method to iteratively conduct material deposition and surface machining to create tall, straight-walled geometries.

1.1.1 Overview of Hybrid Manufacturing (HM)

Hybrid manufacturing (HM) refers to a manufacturing system that utilizes multiple manufacturing methods in combination to produce an end component. With the advancement of 3D printing and rapid manufacturing, methods have generally been broken into three (3) different categories; Additive, Subtractive, and Formative. As depicted in Figure 1.1 [1], each of these categories offers unique setups, process parameters, and accompanying advantages and weaknesses. Combining processes from different categories, most commonly AM with another type of process, enables hybrid manufacturing systems to attain the unique benefits of each category and overcome their individual drawbacks. Often, these different processes are integrated into a singular machine. Many would argue that such integration is a requirement for a system to be considered truly “hybrid”, rather than using separate standalone systems. The processing of reactive materials offers one practical reason for

this— the need for an inert environment exists through all processing steps; using standalone systems would require removing a part from such an environment and re-establishing it on another machine repeatedly [2].

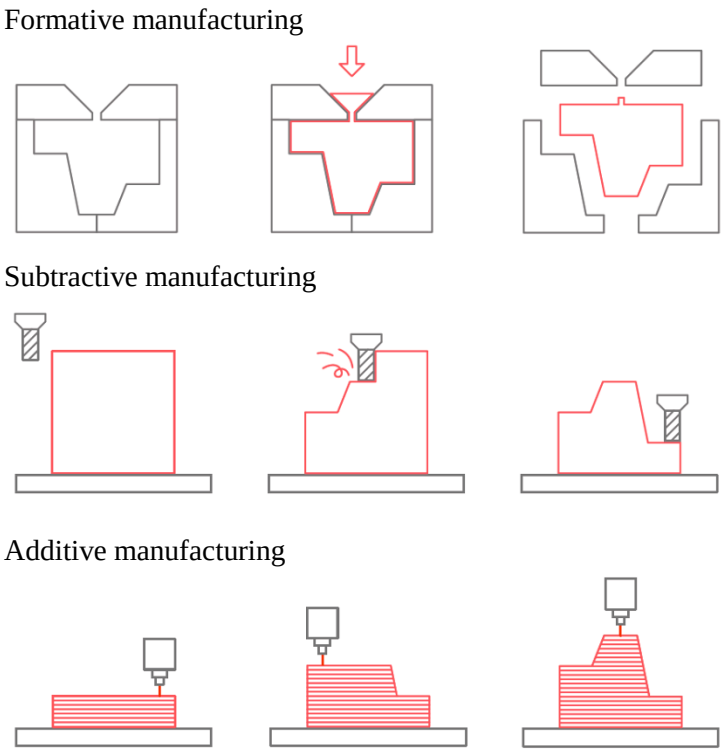

Figure 1.1 Manufacturing method categorization [1]

The combination of additive manufacturing (AM) with CNC machining is often the first combination considered for hybrid manufacturing. These systems have been readily adopted for several industrial applications, including repair applications [3], [4] and functionally-graded or multi-material applications [5]. A significant benefit of using hybrid additive-subtractive manufacturing is the ability to overcome the drawbacks of the individual processes while retaining the best of both processes, as can be seen in Figure 1.2 [6]. Additional benefits to metal AM-CNC hybrid manufacturing systems include 1) a lower overall acquisition cost, 2) a reduced learning curve, 3) enablement of net-shape, 3D-printed, metal parts, 4) speeding the production of complex metal parts, and 5) increasing machine tool

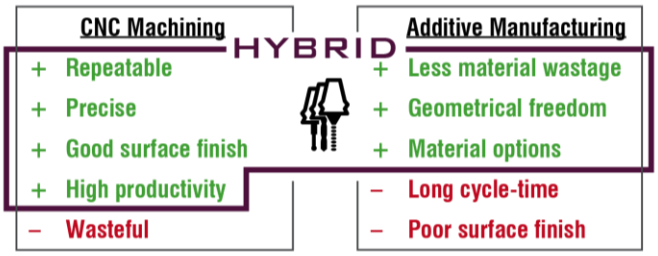

Figure 1.2 Hybrid: the best of both CNC & AM [6]

utilization for repair, coating, and re-manufacturing [7]. Due to their prevalence among industrial HM users, this research will focus on hybrid additive-subtractive manufacturing systems, specifically the combination of DED-AM with CNC machining.

1.1.2 Overview of Directed Energy Deposition (DED)

Directed energy deposition (DED) is a broad terminology for a series of metal additive processes. According to the ASTM/ISO standard for AM terminology (ISO/ASTM 52900-15), 'DED is an additive manufacturing process in which focused thermal energy is used to fuse materials as they are being deposited.' [8]. While there is still some disagreement on which processes would fall under the DED label [1] – [4], this definition would include processes that utilize either a "controlled stream of powder or a wire filament" as the metal feedstock [10]. This includes processes such as 3D laser cladding, direct metal deposition, laser engineered net shaping (LENS), directed light fabrication [11], laser metal deposition (LMD), electron beam additive manufacturing (EBAM) [9], and wire-arc additive manufacturing (WAAM) [12]. Variance of the energy source from process to process also exists within DED, with common sources being a laser, electron beam, or plasma arc [10]. Table 1.1 [10] compares the advantages and disadvantages of these heat sources. This research will focus specifically on laser metal deposition (LMD), a laser-heated, blown-powder variant of DED.

Table 1.1 A comparison of the different heat sources available for DED [10]

	Laser	*Electron Beam*	*Plasma Transfer Arc*
Advantages	Good control over dilution. Low heating of work piece Fiber delivered laser allows for integration into a wide range of platforms	Ability to manipulate the electron beam into multiple beams Cleanliness of a low pressure atmosphere	Lower capital costs, particularly for high power systems
Disadvantages	Lowest efficiency (wall-to-plug) as well as coupling efficiency % Cost of laser significantly increases with power	Requires a low pressure atmosphere which may contribute to high capital cost and long processing time required for evacuation of chamber	Medium to high heating of work piece Difficult to control dilution below 10%

Laser metal deposition produces geometry additively through a laser cladding process. A high-power laser is focused on a surface, creating a melt pool. An inert gas, such as argon, is introduced to shield the melt pool from contamination. Powder feedstock is then blown via an inert carrier gas into this melt pool through small nozzles or orifices to create a material deposition. Movement of the laser with respect to the substrate, or scanning, creates a bead of material similar to the basic welding processes, see Figure 1.3 [13].

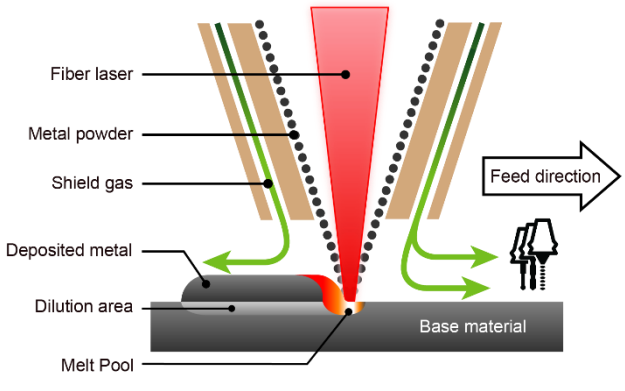

Figure 1.3 Laser metal deposition [13]

The size, depth, and velocity of the resulting melt pool are dependent

upon the laser spot size (determined by laser type, focus, and power), scanning speed, and the energy absorption and thermal conductivity of the feedstock and the substrate. The powder feed rate, the laser scanning speed, and size of the melt pool are all key parameters in determining whether powder enters the melt pool and fuses to the part. Balancing these parameters to create a fast and efficient build presents a challenge to users of DED [8].

Surface finish of parts made with LMD (and DED in general) tends to be fairly rough compared to what is achieved when sand casting or producing parts via a powder-bed fusion (PBF) process. Layer boundaries are often visible, as well as undulations in the surface and a stair-stepping effect on inclined surfaces [14]. The dimensional accuracy of parts is also significantly less than what is possible with a PBF system and generally expected in industrial applications. These imperfections often lead DED to be considered a "near net shape" process rather than a "net shape" process like sand casting or PBF [8]. As a result, it is common to finish the surface of the DED part using CNC machining to attain a suitable surface finish and meet specifications [15]. Figure 1.4 [15] depicts how the intended surface can be attained by first overbuilding a part using DED and then post-processing with a CNC machining process.

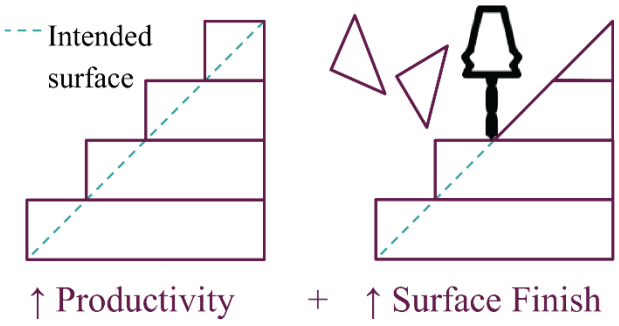

Figure 1.4 Cross-sectional view showing how an overbuilt part can be finished using CNC machining [15]

1.1.3 Process Planning

Machining process planning involves numerous different steps beginning with characterization of the general part shape, determination of stock geometry, feature analysis, setup and fixture determination, and eventually progressing to the selection of tooling and machining parameters. When selecting a machine tool, proper consideration must be given to the tool reach and access. Tool reach is a measure of how far a tool can be extended into a part before colliding with existing geometry (Figure 1.5a) [16]. This is wholly dependent on the length of the tool's stickout. Similarly, tool access refers to the ability of a tool to access a given surface of a part (Figure 1.5b) [16]. This is dependent on the tool diameter and the relationship between two or more vertical surfaces. Machining is ideally conducted using short tools with large diameters. This minimizes the tool's deflection and allows for a more precise surface.

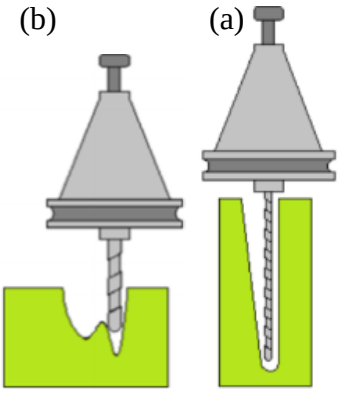

Figure 1.5 Tool reach (a) and access (b) [16]

1.2 Research Problem

A DED-CNC hybrid manufacturing system provides the user with the unique ability to conduct "in-processing finishing of metal AM parts [15]." This along with the ability to produce multi-material components makes this hybrid manufacturing approach rather attractive to users for a variety of applications. An example application is the ability to produce additional geometry on an existing geometric design. For example, the heat sinks and cooling fins could be added to the main

Figure 1.6 Motorcycle engine block with heat sinks and cooling fins [17]

cylinder block of a motorcycle engine, see Figure 1.6 [17]. As can be seen in Figure 1.7, the overall dimensions of the block are greatly expanded by the addition of the cooling fins. However, the majority of this additional volume is absent of material.

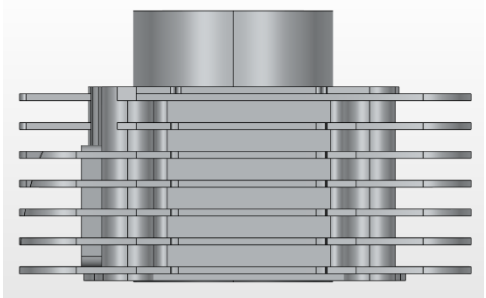

Figure 1.7 Side view of motorcycle engine block

This part is likely produced via a die-casting process that utilizes high pressure to force molten metal into the mold cavity. Current limitations to the die-casting process prevent the creation of extremely tall, thin sections, which limits the designers' ability to create larger cooling fins. Alternatively, if this part were to be machined from raw square stock, there would be a great deal of material waste. As such, this may be an ideal part to create using a hybrid AM-CNC machining system. However, this approach would currently be limited to fin heights that are shorter than the reach of the machine tool used to finish the fin's sides (Figure 1.8). This once again restricts the designer and could require the use of extremely long machine tools.

Tool reach and access problems are not limited to standalone machining; they are equally prevalent in hybrid manufacturing. Machining tall additive features requires the use of long machine tools. As longer machine tools are more prone to deflection, this may lead to a reduction in surface finish quality. The

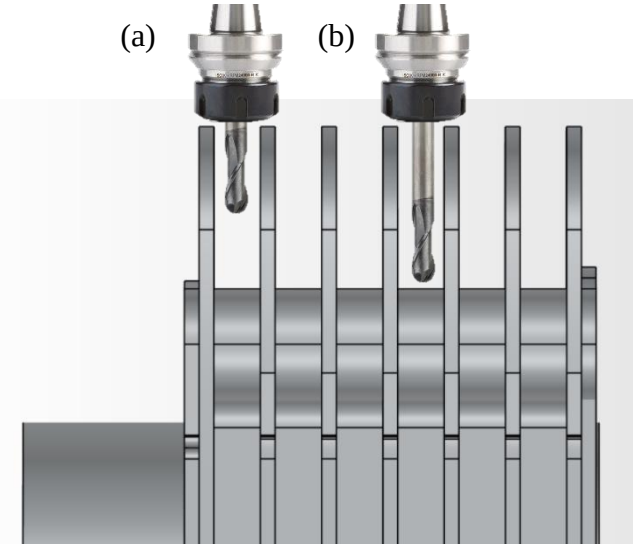

Figure 1.8 Example of tool reach limitations requiring the use of a longer tool (b)

increased deflection experienced from longer tools can be countered by increasing the diameter of the tool. However, this limits the access of the tool to the surface of part. As shown in Figure 1.9, removal of machining allowance can be accomplished on both short features (a) and tall features (b). However, machine tool lengths can quickly become extreme.

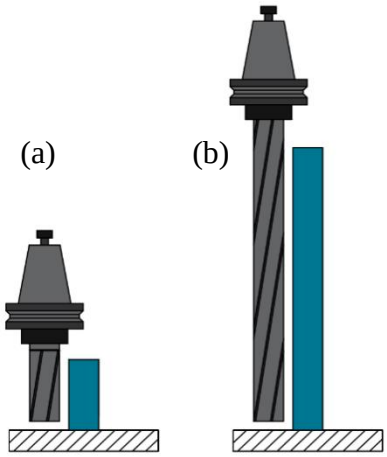

Figure 1.9 Machine tool length comparison

Due to hybrid manufacturing's unique ability to perform iterative deposition and machining, tall features can be broken down into several shorter features (Figure 1.10). Breaking tall features down into shorter features and performing machining in stages enables the use of shorter machine tools. Machining however, being a material removal process, can present an issue for subsequent depositions. Like other additive processes, DED is a layer-based process. Similarly, material can only be added where support exists for the deposition. Therefore, a support angle, θ, is necessary to expand beyond the bounds of the machined geometry's top plane (Figure 1.11). This support angle prevents the machining allowance from being fully attained on the initial layers of subsequent depositions after it has been removed, unless the angle is 0 degrees. For instance, a support angle of $\theta = 45°$ would equate to a section of material with less than desired machining allowance as tall as the machining allowance is

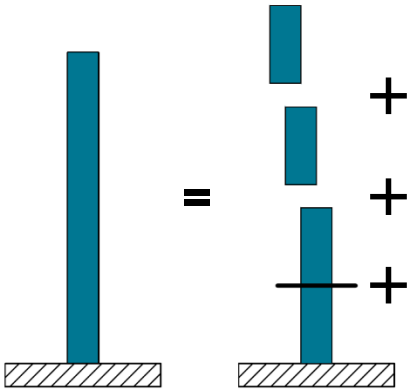

Figure 1.10 Breaking down tall features

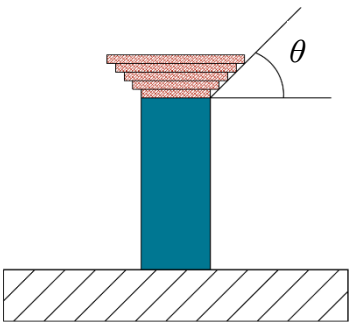

Figure 1.11 Support angle

wide. This is problematic as the machining allowance is critical in attaining the final part's specified surface finish. A method to continuously cycle between deposition and machining without sacrificing machining allowance is necessary to progress hybrid manufacturing in the production environment.

1.3 Research Objectives

We lack a formal automated process planning method for a hybrid manufacturing system using additive manufacturing with 3-axis CNC machining. Specifically, we lack a method to handle reach and access when multi-axis orientation is not possible. This research takes the first steps toward the creation of such a process planning approach. The three (3) major objectives of this research are:

1) To develop a method for the creation of straight-wall geometry that exceeds the reach of a milling tool in the presence of access restrictions due to nearby geometry.
2) To investigate the requirements for machining allowance material to act as a support structure, given parameters for both the additive and subtractive conditions and limitations.
3) To implement the developed method in a hybrid manufacturing system using laser metal deposition (LMD) and 3-axis CNC machining.

1.4 Thesis Organization

The remainder of this thesis is organized as follows— Chapter 2 will review existing hybrid manufacturing systems that perform iterative operations as well as the current support structures for metal AM processes. Chapter 3 will describe the iterative method and its development process. Then, Chapter 4 will present the implementation of such a method to create a representative geometry. Finally, Chapter 5 will present the conclusions of this thesis and opportunities for future work.

CHAPTER 2. LITERATURE REVIEW

The concept of iterative hybrid manufacturing is not a new one. Solid ground curing (SGC) developed by Cubital in Israel, utilizes a UV-cured, liquid resin to create part geometry and wax as a support structure. Each is deposited on a given layer before the whole layer is machined to a given thickness [18]. Similarly, multi-jet modeling developed by Sanders, et. al. [19], commercially available from Solidscape, Inc. [20], deposits both build and support wax materials using drop-on-demand technology into the build envelope before precisely milling each layer. While these processes utilize deposition and machining iteratively, the wax support structures are not capable of supporting metal depositions.

Shape deposition manufacturing (SDM) produces metal shapes utilizing an iterative, HM approach combining microcasting (a weld-based deposition process), 5-axis CNC machining, and shot-peening. Complex parts are broken down into layers of arbitrary thickness to allow the part to be made with simple operations. Each layer height is determined by local geometry, segmenting parts by feature type. Layers are grouped into three different feature types, non-undercuts, undercuts, or both (Figure 2.1, [21]) . Each layer contains a machining cycle to machine the build surface of the part (Figure 2.2b, [21]), create a cavity for deposition (Figure 2.2f, [21]), or both (Figure 2.3, [21]). Layers containing both undercut and non-undercut features are segmented to place undercut features next to areas with previous deposition. Build and support material can vary for SDM, with metal AM having been conducted with stainless steel as the build material and copper as the support material. Shot-peeing is conducted between

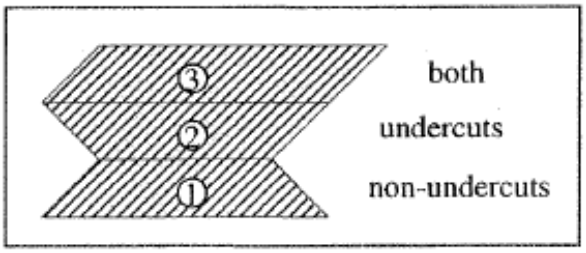

Figure 2.1 Arbitrary segmentation of layers based on local geometry in SDM [21]

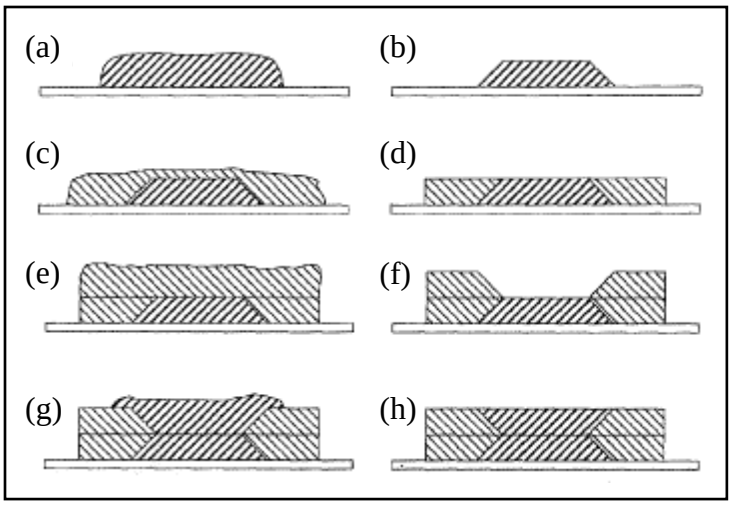

Figure 2.2 Shape deposition manufacturing of:

Non-undercut features: (a) deposition of build material and (b) shaping of build before (c) deposition of support material and (d) planing the top surface

Undercut features: (e) deposition of support material and (f) shaping of support material before (g) deposition of build material and (h) planing [21]

layers to control the build-up of stresses within the part [21]. SDM is capable of producing metal components via an iterative HM process; however, this process relies on complex, 5-axis toolpaths and multi-material deposition. Additionally, complex part segmentation is necessary to separate features into undercut and non-undercut features for a given layer.

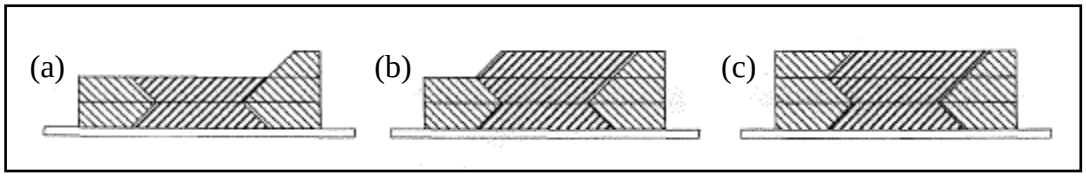

Figure 2.3 Shape deposition manufacturing of layers containing both undercut and non-undercut features; (a) deposition and shaping portions of the support material, (b) deposition and shaping of build material, and (c) deposition of remaining support material and planing the top surface [21]

Integration of metal powder bed fusion with CNC milling, such as the HM system presented by Matsuura [22] provides a metal AM system with a precision machining center. However, the passive support of the powder bed is insufficient to prevent part distortion and additional supports are required. The removal of these structures requires a further post processing operation that often requires additional fixturing or machine setups. [23] details a

complex lattice support structure system (Figure 2.4) that attempts to minimize the volume of these support structures and their connection to the part. Other integrations of metal AM process with CNC machining centers exist, such as laser cladding [24], [25], LENS [26], laser deposition welding [27], and WAAM [12]. These systems face issues with the creation of support structures and users often seek to avoid them through multi-axis part orientation or material deposition [28]–[30]. To date, no HM system has used metal AM in combination with 3-axis CNC machining to produce components presenting reach and access restrictions without the addition of dissimilar support materials, further post-processing, or multi-axis part orientation.

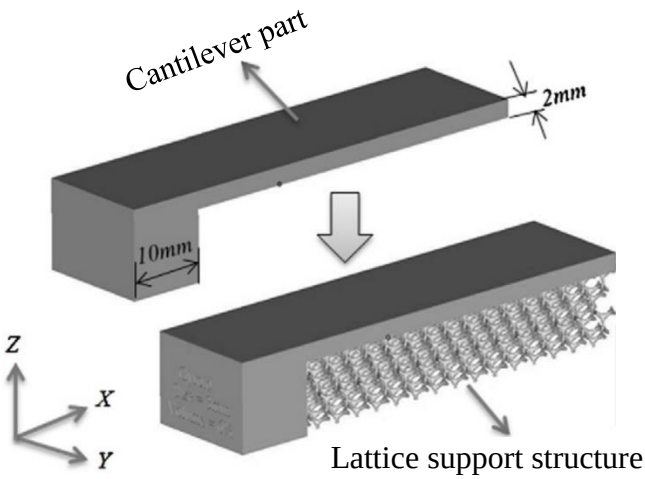

Figure 2.4 Lattice support structure on a cantilever part [23]

CHAPTER 3. METHODS

The following chapter introduces a 3-axis, computer numerical control (CNC) machining method that when utilized in a hybrid manufacturing (HM) system is capable of 1) creating tall, straight-walled geometries, 2) managing the removal of machining allowance (MA) material under reach and access restrictions where multi-axis orientation is not possible, and 3) maintaining support structures for subsequent depositions while conducting material deposition and removal iteratively.

3.1 Method Overview

Following deposition of material via an additive process, the exact surface geometry of a component is unknown. Hybrid manufacturing often integrates post-processing in the form of machining or another finishing process to achieve final part tolerances. The following method takes this a step further, integrating machining mid-process.

First, a tall component is broken into smaller, shorter sections referred to as *slabs* within this paper. Each slab is essentially treated as a separate component with a deposition cycle and a machining cycle. Face milling is conducted between deposition cycles to eliminate inconsistencies in the stack up of the 2-½ D layers and provide a known flat surface. Profile milling is also conducted along the contour of the part, removing any excess material and selected portions of the machining allowance. This process continues iteratively, generating slabs of material until the final height of the part is attained.

This process is unique in that profile milling is not conducted with standard flat or ball end mills; rather, side or undercut machine tools are used. These cutting tools allow for material to be removed from the side or below rather than from above– even in a simple three-axis machine setup. Leveraging side-cutting tools, a ledge is created by selectively

removing the machining allowance from the bottom up. The created ledge then acts as a support structure for additional material to be deposited in subsequent additive cycles.

3.1.1 Process Flow

Figure 3.1 depicts the desired geometry for a tall, straight-walled component Figure 3.1a, and then the process flow for an iterative hybrid manufacturing process. This process repeatedly cycles between deposition of material via an AM process and material removal via CNC machining. The process starts with a short material deposition, oversized by an appropriate machining allowance, Figure 3.1b. This is followed by a two-stage machining cycle, beginning with face milling, Figure 3.1c, before transitioning to profile milling and creation of the ledge, Figure 3.1d. These three steps— 1) deposition, 2) face milling, and 3) profile milling are repeated, Figure 3.1e-i, until the final desired height is attained.

Utilizing the novel support structure of the ledges (Figure 3.1d) allows for the practical creation of tall, straight-walled features. The same short machine tools can be used for all iterations of the process regardless of the overall height of the part. Further relaxation of machine tool requirements occurs on the final profile milling iteration. With no further depositions to occur, the support of a ledge is no longer required to create, and, therefore, nor are the

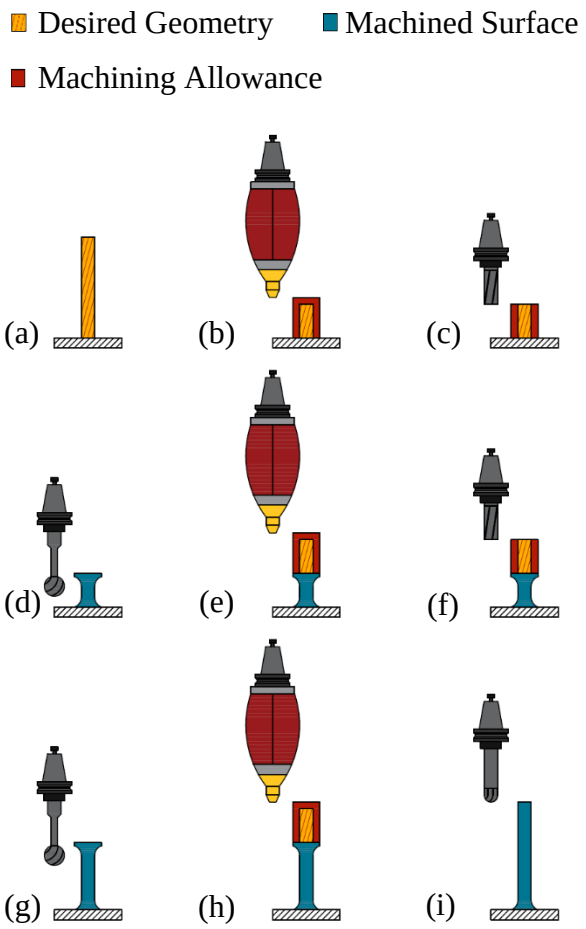

Figure 3.1 Process flow for iterative hybrid manufacturing

undercut machine tools to create the ledge. This allows the user to conduct the final profile milling using a standard ball, or even flat, end mill, see Figure 3.1i.

3.1.2 Undercut Machine Tools

Undercut machine tools provide the unique ability for material to be removed from the side or below rather than above a component, providing access to surfaces not visible from the spindle. As their name implies, these tools create undercut, or overhanging, features within a component. Figure 3.2 [31], [32] depicts common examples of undercut machine features, including a t-slot and dovetail. These features are generally described by their depth and width, and, in the case of a dovetail, the angle. The use of undercut machine tools is particularly advantageous as the creation of similar features via an additive process would require the use of support structures and appropriate support angles.

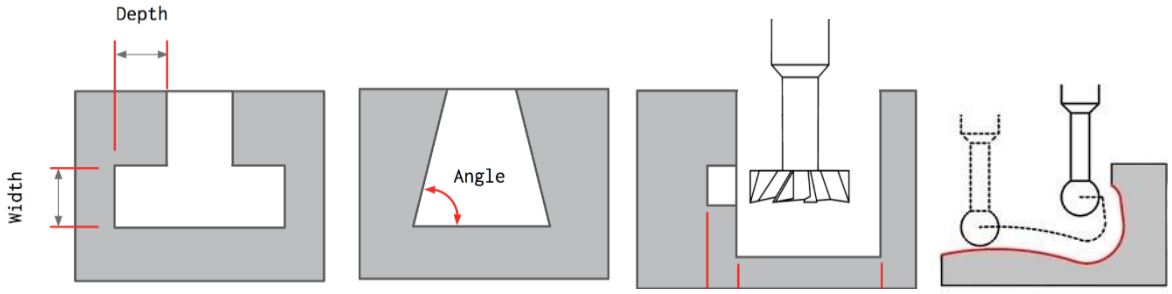

Figure 3.2 Common undercut machine tooling features (adapted from [31], [32])

To allow the cutting portion of the machine tool to access the part without collision, these tools have a shank with a reduced diameter in comparison to the cutting geometry (Figure 3.3). The undercut machine tool utilized in this machining method is a spherical ball end mill, colloquially referred to

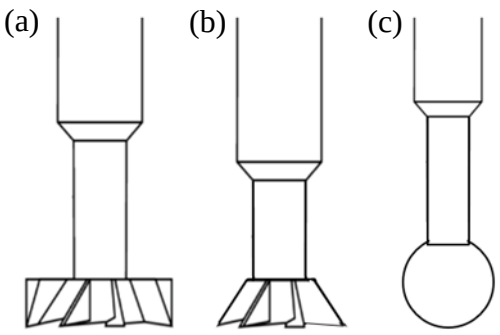

Figure 3.3 Undercutting machine tools: (a) t-slot cutter, (b) dovetail cutter, and (c) lollipop endmill

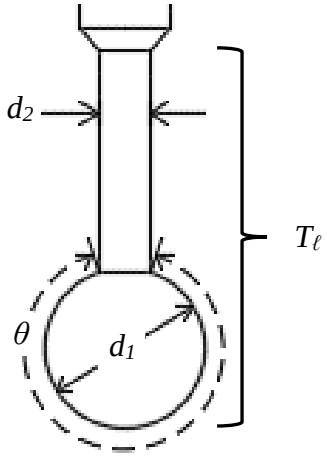

Figure 3.4 Lollipop endmill geometry

as a "lollipop" end mill. Figure 3.4 depicts the geometric parameters that describe this tooling, where T_ℓ is the effective length (or reach) of the tool, d_1 is the diameter of the cutter, d_2 is the reduced diameter of the shank, and θ is the wrap angle (or included angle), designated in degrees relating the two diameters. Standard tools are available in 220°, 270°, and 300° options.

3.2 Process Parameters

This section will detail the key parameters involved in the processing method presented above. The relationship between these parameters will be discussed in detail at the end of the section. Table 3.1 lists the process variables and their symbolic representation.

Table 3.1 Process variables and their symbolic representations

Symbol	Process Variable
A_s	slab allowance
α	ledge thickness
β	ledge overhang
D	distance between features
d_1	cutter diameter
d_2	tool shank diameter
ε_ℓ	error in layer height
H_C	final component height

Symbol	Process Variable
h_ℓ	layer height
H_R	resulting slab height
H_S	slab height
n	number of layers per slab
m	number of slabs per component
R	ledge radius
T_ℓ	tool reach (tool length)
θ	cutting tool's included angle

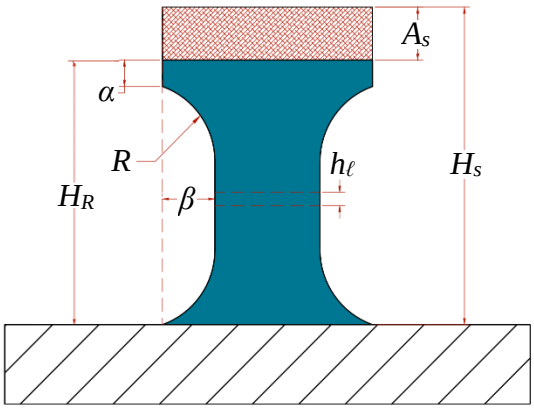

Figure 3.5 Process parameters

Figure 3.5 lays out some of the most prominent parameters used to define the outlined process. This process begins with segmenting a component into shorter sections referred to as *slabs*. Slab are stacks of numerous 2 ½-D cross-sections, known as *layers*. Layer height, h_ℓ, refers to the height of an individual layer, while the slab height, H_s, refers to the overall height of the stack for a given deposition cycle. The slab allowance, A_s, refers to the height of material that face-milling removes from the top of the part. The resulting height of the slab, H_R, is the difference of slab height and allowance. Not pictured, the final component height, H_C, is attained after all slabs have been deposited and machined. The overhanging portion of the machined slab will be referred to as the *ledge*. The ledge can be described geometrically by three key parameters: 1) the thickness of the ledge at its narrowest point, α, 2) the distance which the ledge protrudes from the feature's machined side, β, and 3) the radius sloping down from the ledge to the feature's flat side, R.

These parameters are all interconnected but can loosely be grouped into one of two categories; deposition parameters and machining geometry parameters. Layer height and slab height are characteristics that are inherently closer to the deposition process. Meanwhile, ledge thickness, overhang, and radius are almost exclusively determined by the machining process. Slab allowance is a characteristic that can easily be related to both categories. As the deposition process precedes machining in this method, the deposition parameters will be considered first.

3.2.1 Slab Height (H_s)

The slab height or the height of a single deposition cycle is determined by considering several process attributes. The main goal in decomposing tall geometries into smaller slabs is to enable the use of shorter machine tools; thus, tool reach (the ability of a tool to extend into a part without collision) is the first factor that must be considered. Generally, the easiest way to increase tool reach is to increase tool length. For this reason, throughout the rest of this paper, tool length and tool reach will be used interchangeably. As the reach is dependent upon the depth of machining required, the overall slab height must be less than the reach of the shortest machine tool used to machine the contour of the slab. Eqn. 3.1 describes this relationship, where T_ℓ is the length (reach) of a given tool and H_s is the slab height.

$$H_s \leq min\{T_\ell\} \quad \text{Eqn. 3.1}$$

3.2.2 Layer Height (h_ℓ)

Layer height is the intended height of an individual layer within an additively-manufactured component. This parameter cannot be set directly, and the actual layer height depends on the AM processing parameters (Eqn. 3.2). More accurately, layer height describes the height of the 2 ½-D cross-sections that a component is segmented into when generating machine code. For this process planning method, the component is a slab of height H_S , which will be segmented into n layers of height h_ℓ (Eqn. 3.3).

$$h_{\ell_{actual}} = h_\ell + \varepsilon_\ell \quad \text{Eqn. 3.2}$$

$$H_s \approx n * h_\ell \quad \text{Eqn. 3.3}$$

As previously mentioned, the layer height is highly dependent upon the AM processing parameters. In the case of laser metal deposition (LMD), selection of laser scanning speed, powder feed rate, and laser power all have a large impact on the actual layer height. While the layer height itself doesn't directly impact the success of this HM method,

the error in each individual layer does. While each layer has unique errors and inconsistencies, repeated errors stacked upon themselves quickly become problematic. Layer height should be selected or targeted to minimize the accumulation of error per a given slab height. Eqn. 3.4 describes the relationship between the slab height H_s , layer height h_ℓ , number of layers n, and the error in the i^{th} layer height, $\varepsilon_{\ell[i]}$. Such a selection is beyond the scope of this research, as it is highly dependent on the AM process being employed. Additional impacts of the layer height are discussed in 3.2.6.

$$H_{S_{actual}} = n * h_\ell + \sum_{i=1}^{n} \varepsilon_{\ell[i]} \qquad \text{Eqn. 3.4}$$

3.2.3 Slab Allowance (A_s)

The slab allowance is the machining allowance of a given slab that will be removed during the face-milling phase. The purpose of the face-milling phase is to remove any undulations and irregularities within the top surface of the deposition caused by the buildup of errors within the individual layer heights (Eqn. 3.5). Once complete, a known, flat surface exists as a foundation for future depositions. This process step imitates the work of solid ground curing [18], shape deposition manufacturing [21], and multi-jet modeling [19]. The slab allowance, therefore, must be sufficiently large to ensure a flat surface when removed regardless of the actual surface profile. Eqn. 3.6 quantifies the resultant component height, H_R , with respect to slab height, H_S , and slab allowance, A_S (Figure 3.6).

$$A_s \geq \sum_{i=1}^{n} \varepsilon_{\ell[i]} \qquad \text{Eqn. 3.5}$$

$$H_R = H_S - A_s \qquad \text{Eqn. 3.6}$$

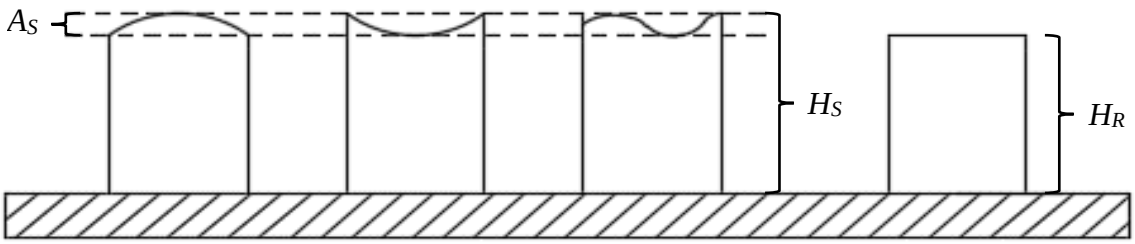

Figure 3.6 Relationship of slab allowance, slab height, and the resultant slab height

3.2.4 Ledge thickness (α) and ledge overhang (β)

The ledge thickness and overhang are largely independent of the previous deposition, excluding the fact that they cannot exceed the geometric volume of said deposition (Figure 3.7). It is recommended that the ledge overhang be held constant throughout a geometry's contour, indicated by the dashed line in Figure 3.7. Independence from the previous deposition allows the user a great deal of flexibility within setting these parameters.

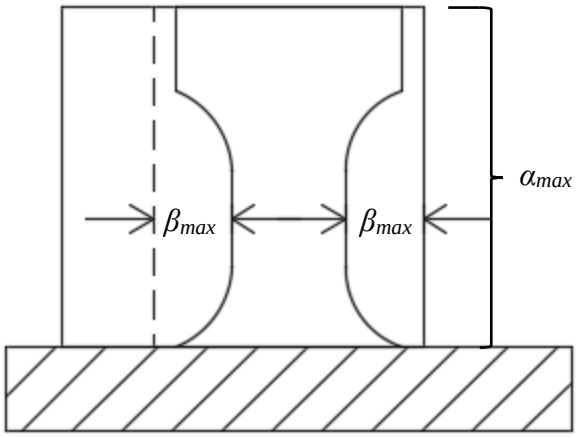

Figure 3.7 Constraint of ledge thickness and overhang

The ledge thickness and overhang parameters should be set at levels to provide desirable outcomes in subsequent depositions. Specifically, the ledge thickness must be sufficiently large enough to support the next deposition cycle and the ledge overhang must be sufficiently large to provide an adequate machining allowance on the next deposition. As such, these two parameters are not considered when no ledge is created, i.e. the final machining cycle; the final slab of the component is simply machined to the specified dimensions.

When selecting the ledge thickness, the user needs to be conscious of the parameters for the next deposition cycle, particularly laser power and scanning speed. A given ledge, i.e. amount of material, can only withstand a certain heat (energy) input before softening, sagging, melting, or even, being vaporized. Such conditions may deteriorate the ledge's ability to support subsequent layers and potentially render the support structure ineffective. It is anticipated that excessively thin ledges will be at risk of melting/vaporizing and increasing the ledge thickness will allow for more heat input before such conditions occur. However, as the thickness of the ledge increases, the length of the machining tool required to remove the ledge on the subsequent machining operation increases (Figure 3.8).

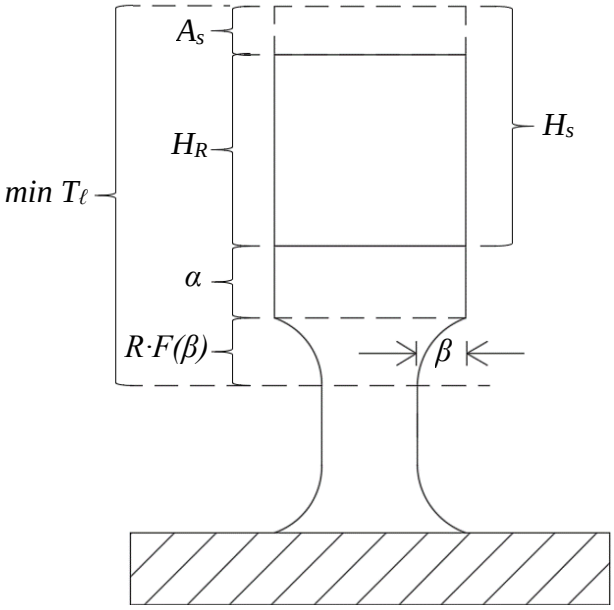

Figure 3.8 Impact of the ledge thickness on minimum tool length

Eqn. 3.7 describes the relationship between tool length T_ℓ , ledge height, and the vertical component of the ledge radius R (discussed in the following section 3.2.5), where $F(\beta)$ is a function of β. To minimize tool length, one should seek to minimize the ledge thickness while adhering to constraints related to heat input. It should be noted, however, that this is not a critically important concern as the ledge thickness is an order of magnitude smaller than the tool length and slab height.

$$T_\ell \geq (H_R) + \alpha + R * F(\beta) \qquad \text{Eqn. 3.7}$$

3.2.5 Ledge Radius (*R*) and Tool Radius

The ledge radius is highly correlated to the radius of the machining tools, specifically the lollipop cutter. Due to the complexity introduced by differing the tool radius and the ledge radius, the two will practically be considered the same. This relationship is described explicitly in Eqn. 3.8, where d_1 is the diameter of cutter geometry.

$$R = \frac{d_1}{2} \qquad \text{Eqn. 3.8}$$

Additionally, the tool radius must be selected with the machining allowance in mind, as the machining allowance cannot exceed the tool radius. The ledge overhang, tied closely to machining allowance, cannot exceed the ability of the tool to reach the side of the part without colliding the shank with the deposition. The lollipop endmill offers an advantage here, as its geometry is characterized by a reduced diameter shank, d_2. Eqn. 3.9 describes this relationship, where d_1 is the diameter of the cutter and d_2 is the reduced diameter of the shank. This relationship is also depicted in Figure 3.9.

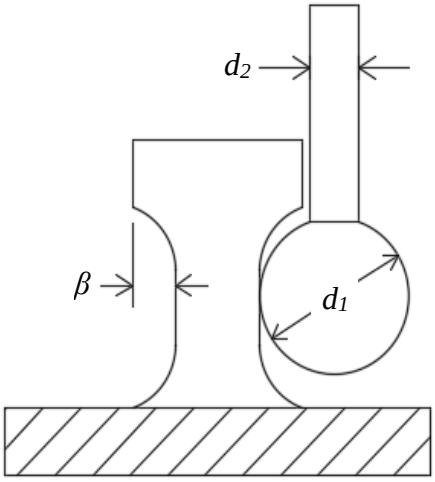

Figure 3.9 Comparison of tool diameters to ledge overhang

$$\beta \leq (d_1 - d_2)/2 \qquad \text{Eqn. 3.9}$$

Another key consideration that must be made when selecting the tool radius is the ability of the tool to access the required geometry, particularly as geometries become more complex and include multiple features. Under conditions where access is constrained by multiple features,

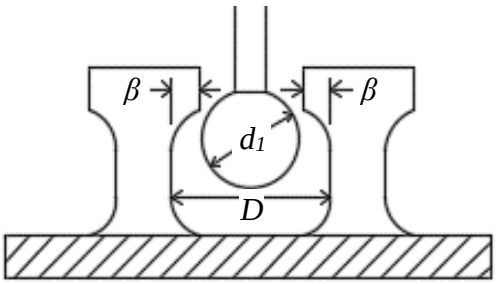

Figure 3.10 Matching tool diameter to the distance between features

the tool radius is constrained by Eqn. 3.10, where D is the distance between two features, d_1 is the diameter of the cutter, and β is the ledge overhang (Figure 3.10).

$$D \geq d_1 + 2\beta \qquad \text{Eqn. 3.10}$$

3.2.6 Number of slabs (m) and final component height (H_c)

The number of slabs required to reach a final component height depends on the resultant height of the individual slabs following the removal of the slab allowance (Figure 3.11). The resultant component height is the effective contribution of a slab to the final component height. Eqn. 3.11 describes this relationship, where H_C is the final component height, m is the number of slabs, and $H_{R[j]}$ is the resultant height of the j^{th} slab.

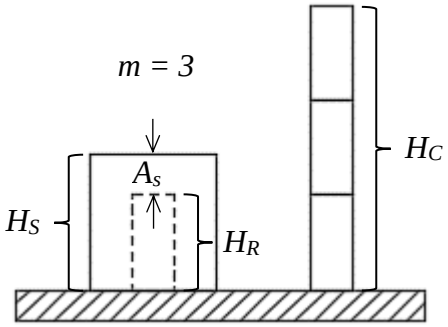

Figure 3.11 The relationship of component, slab, and resultant heights, including slab allowance

$$H_C = \sum_{j=1}^{m} H_{R[j]} \qquad \text{Eqn. 3.11}$$

$$\#\ of\ changeover\ cycles = m - 1 \qquad \text{Eqn. 3.12}$$

Iterative hybrid manufacturing requires switching from deposition to machining (and vice versa). The cost of this changeover cycle is a key factor in the selection of m due to the relationship described in Eqn. 3.12. This cost includes both a fixed and variable portion. The fixed cost is associated with the changeover of a hybrid system from one manufacturing method to another. This cost is largely realized as the time it takes to change the system over, as well as the resources consumed, such as flow and cover gas, metal powder and energy. This cost is inherent to a given hybrid system and not impacted by the design of the proposed method. The variable cost of switching, on the other hand, is highly related to the proposed

method, particularly the machining allowances and the frequency with which they are removed.

The machining allowances in this process planning method, namely the slab allowance and the ledge overhang, like any other machining allowances, are considered waste with respect to the overall process. As such, it is desirable to minimize them. However, the purpose of these allowances is to overcompensate for any variation within the additive or formative process while also encapsulating the desired geometry. Therefore, as a component's cross-section increases, so does the volume of material within the machining allowance (Figure 3.12). A similar phenomenon exists when the slab allowance is increased; however, this exhibits itself in the volume generated by the interaction of the slab allowance and ledge overhang (Figure 3.13). These increases in the size of the part's cross-section or the slab allowance create additional volumes of material that must be removed during the face-milling portion of the machining cycle. This increases the waste of the process and the amount of material that must be re-deposited, an issue that is only compounded as the number of slabs increases.

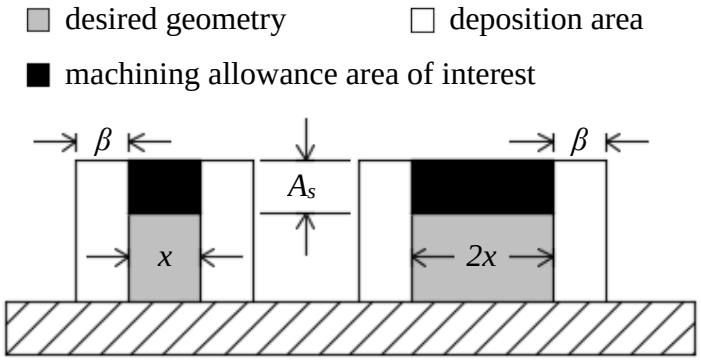

Figure 3.12 Growth of slab machining allowance with an increase in a cross-sectional dimension of the component

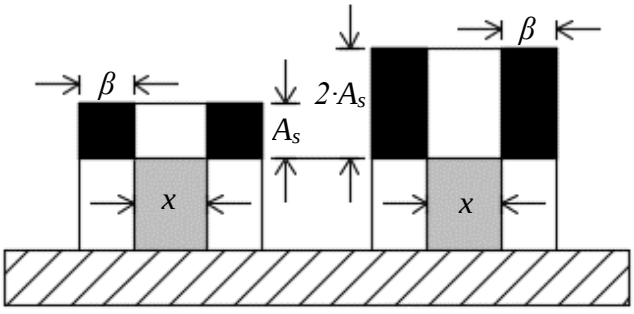

Figure 3.13 Growth of machining allowance with an increase in slab allowance

Numerous factors contribute to raw material and processing costs, production time, and the overall waste of this process. Slab height, slab allowance, and their resultant slab height could all be used to "optimize" the process to produce minimal waste or incur minimal raw material cost. The number of slabs could be used to optimize production time by minimizing the time spent on changeover cycles. Any of these parameters, however, are intricately tied to numerous other parameters. The proper balance or selection of parameters ultimately depends upon the user's definition of optimization, be it speed, cost, waste, or some other metric. This thesis will only include a preliminary exploration of the implications of two (2) parameters, ledge thickness (α) and ledge overhang (β), on the remainder of the process, as presented below.

3.3 Parametric Evaluation

This method of iterative hybrid manufacturing relies on the ability to effectively create and remove material. Therefore, both successful material deposition via additive manufacturing and material removal via a subtractive process are required; without each inhibiting the other. For this particular method, it relies on the ability to complete the material removal process while leaving appropriate material for subsequent depositions. Therefore, the parameters surrounding the ledge's geometry and its functionality will be considered for further investigation.

3.3.1 Motivation to Evaluate Ledge Thickness

Numerous parameters should be balanced during the process planning phase of the proposed hybrid manufacturing method. It is believed that of these parameters, those associated with the ledge's geometry will have the largest impact, particularly the ledge's thickness.

Parameters such as the distance between features, the final component height, individual slab height, and the required machining allowance are useful for identifying a tool's required reach and the ability to access geometry. As such, these parameters are useful for selecting tool length, tool diameters, and the included angle of the lollipop cutter and other machine tools. However, this selection is dependent on the geometry of the part being created and primarily drives success in the machining stages of the process. Cut depth and width are dependent upon the machine tools being used, the material being processed, and the specifications of the end component. An experienced machinist is capable of driving success in the machining stages of the process. Similarly, parameters such as layer height, slab height, and slab allowance are highly dependent on the deposition process and its accumulation of error. The selection of these parameters, therefore, drives success in the additive portion of the manufacturing method. However, a successful interface between the additive and subtractive portions of the process is critical to the overall success of the method. Therefore, focus was given to the parameters associated with the ledge's geometry.

The main parameters describing the ledge's geometry include ledge thickness (α), ledge overhang (β), and ledge radius (R). Of these parameters, ledge thickness was hypothesized to have the highest probability of impacting the success of the method. Ledge overhang essentially acts as a machining allowance and is dependent on the user to implement appropriately for their machining process and specifications. To evaluate the ledge's functionality, the ledge overhang was set at a common machining allowance value of 0.025" (0.635 mm). Ledge radius is highly correlated with the radius/diameter of the cutting geometry of the spherical ball end mill. The selection of this diameter is depended on the distance between features and the ledge overhang (machining allowance) necessary. These

parameters are highly dependent on the geometry and specifications of the end component. Ledge thickness, however, is a relatively independent parameter that can be critical in determining the ability of a ledge to support subsequent depositions. The support capability of thin ledges is of particular interest, as they may fail to withstand the heat and weight of the following deposition cycle. Therefore, ledge thickness was investigated further to determine its impact.

3.3.2 Experimental Design

To investigate the impact of ledge thickness (α) on subsequent depositions, a small experiment was conducted. Three samples were created at different levels of α— 0.000" (0.00 mm), 0.005" (0.127 mm), and 0.010" (0.254 mm). All other parameters were held constant, including ledge overhang, β, which was set to 0.025" (0.635 mm) for all three trials. Table 3.2 details the parameters used during the experiment.

Table 3.2 Parametric description of ledge thickness experiment

Process Variable	Set Level	
	Metric	Standard
laser power	*300 Watts*	
travel speed	*650 mm/min*	*25.59 in./min*
powder feed rate	*3.1 g/min*	*0.11 oz/min*
carrier gas flow	*4.0 L/min*	*0.14 CFM*
shield gas flow	*8.0 L/min*	*0.28 CFM*
laser spot size	*1 mm*	*0.0394 in.*

Process Variable	Set Level	
	Metric	Standard
standoff distance	*10 mm*	*0.3937 in.*
layer height	*0.2159 mm*	*0.0085 in.*
slab height	*6.35 mm*	*0.250 in.*
tool reach	*12.26 mm*	*0.483 in.*
tool radius	*3.18 mm*	*0.125 in.*
included angle	*300°*	
shank diameter	*3.18 mm*	*0.125 in.*

To prepare samples, a hot-rolled 316L stainless steel bar was machined to form a representative component with a machined ledge. Utilizing DED-AM, eight (8) layers were deposited on top of the ledge, each rotating 90° from the last layer. Toolpaths began in one corner of the part and zig-zagged over the entire cross-section to eventually complete

deposition on the opposite corner. Figure 3.14 depicts the toolpath of the initial layer of deposition. As can be seen, the deposition path positions the center of the weld bead was just inside of the edge of the desired geometry. Additionally, the specimen's dimensions were selected so that an integer number of beads could be deposited on each layer; in the case of the initial layer, 11 equally spaced beads cover the entire cross-section of the sample evenly. The same machine code was used for deposition on all three samples.

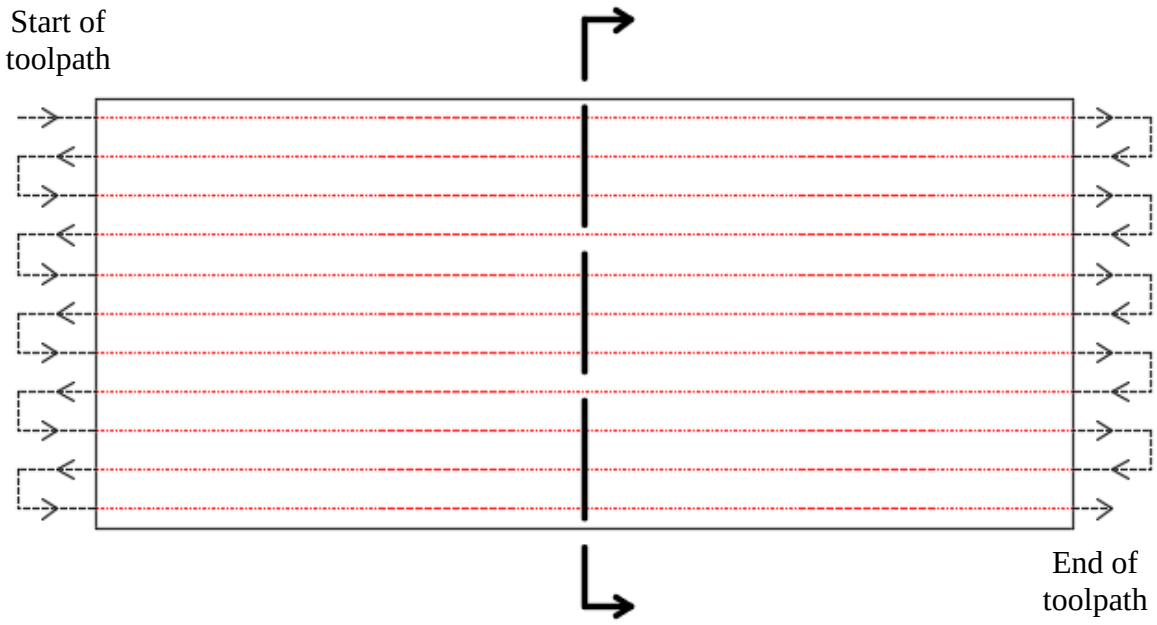

Figure 3.14 Deposition toolpath for the initial layer of all specimens

Using a precision sectioning saw and diamond wafering blade, samples were cross-sectioned perpendicular to the direction(s) of the initial toolpath. Following standard metallography practices, samples were mounted and polished. All specimens were mounted such that the initial pass of the toolpath is on the left-hand side of the sample, while the final weld bead is on the right. The direction of this cross-section is visible in Figure 3.14. Using a digital microscope, images of the samples were captured and then pieced together using the merge functionality of Adobe® Photoshop®, see Figure 3.15 - Figure 3.17.

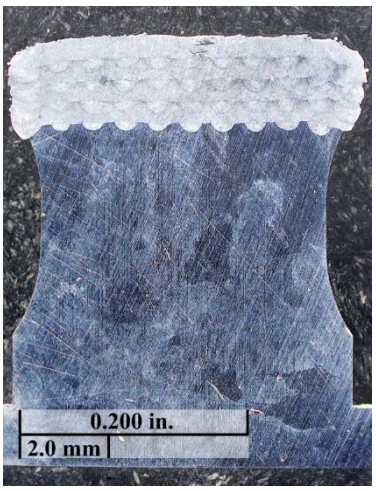

Figure 3.15 alpha = 0.000” (0.000 mm)

Figure 3.16 alpha = 0.005” (0.127 mm)

Figure 3.17 alpha = 0.010” (0.254 mm)

3.3.3 Experimental Results

Measurements of each sample were taken according to Figure 3.18. Using machined reference features, the location of the top surface of the machined ledge prior to deposition was identified as a datum. The expected component height was then identified by adding the expected layer height to this datum surface eight times. Additionally, the original edges of the machined ledge were located as datum surfaces. Measurements A1 and A2 correspond to the deviation from this expected component height at the left and right side of the machined ledge respectively. B1 and B2 similarly correspond to the weld depth at the left and right side of the machined ledge respectively. For comparison, the weld depths of the remaining beads were measured, and the average was calculated.

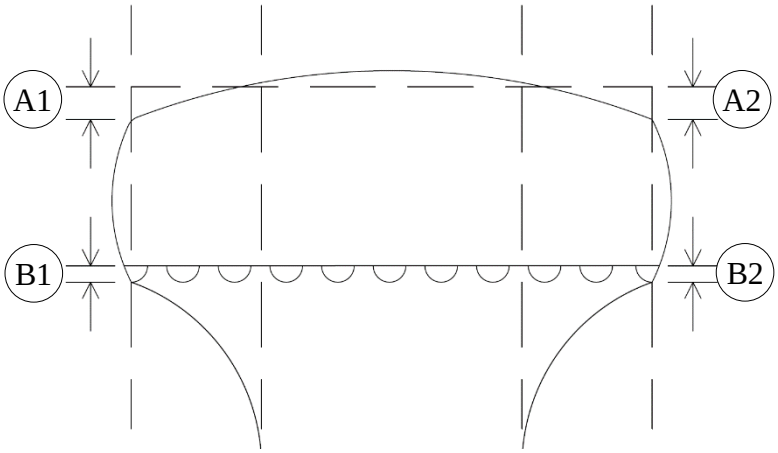

Figure 3.18 Location of measurements

The resulting deviation from the expected components' heights showed no apparent trends (Figure 3.19). The values for either side (A1 or A2) are not consistently larger than the other. Additionally, values were comparable from specimen to specimen, with values ranging from -0.0098 to -0.0194 inches (-0.249 to -0.493 mm) and averages ranging from -0.0127 to -0.0147 inches (-0.321 to -0.372 mm). These negative values indicate that the height at the edge of the component was less than the expected height— an undesirable result.

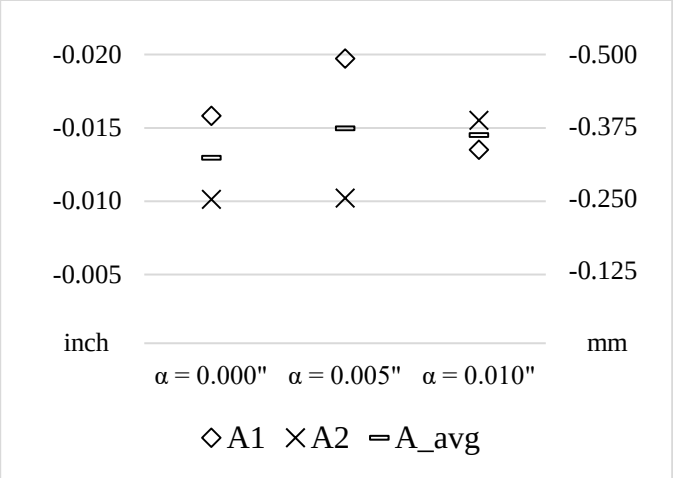

Figure 3.19 Deviation from expected component height

Figure 3.20 depicts the measured weld depths for each of the weld beads as you move across the specimen from left to right. The movement corresponds with the progress of the

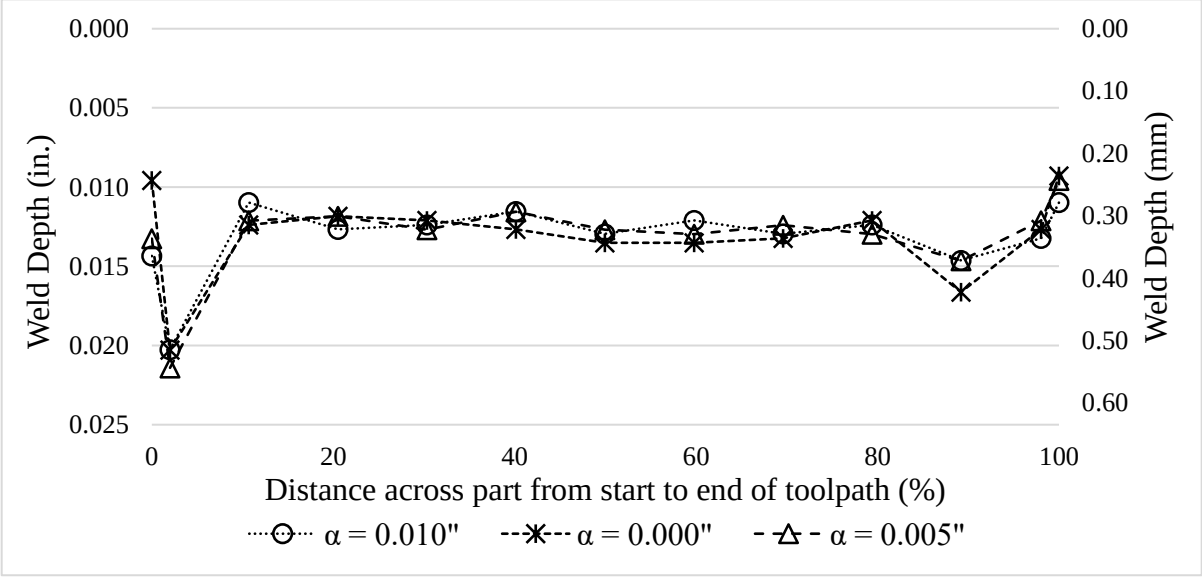

Figure 3.20 Weld depth from B1 (left) to B2 (right)

deposition toolpath, as the rightmost weld bead was the last to be deposited. Upon measurement of the samples, it was discovered that the weld depth was not greatest at the locations corresponding to B1 and B2. The weld beads on the edge, the same weld beads containing B1 and B2, saw further penetration into the radius of the ledge. This increased penetration is comparable for all ledge thicknesses. Additionally, it was noted that the second from the right weld bead saw further penetration than the rightmost weld bead (containing B2) on all samples. This could be due to the buildup of heat in the part as the deposition progressed from side to the other.

Ledge thickness does not appear to have a significant impact on weld depth. Figure 3.21 highlights how weld depth compares across the different ledge thicknesses. The average weld depths are extremely similar at 0.0131, 0.0126, and 0.0126 inches (0.332, 0.320, and 0.320 mm). The average was calculated using from the measured depth of the interior weld beads, i.e. excluding the weld beads that contain B1 and B2. The maximum weld depth was similarly identified, with the α=0.000 specimen having the largest maximum.

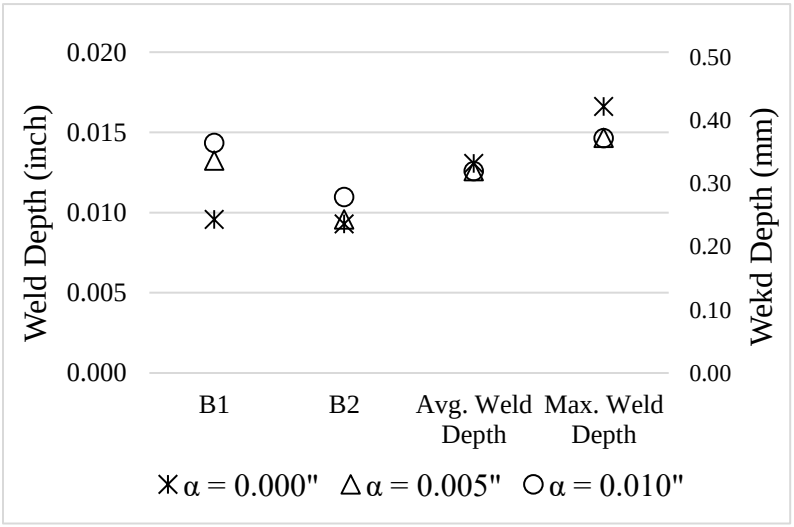

Figure 3.21 B1 and B2 compared to average and maximum

Additionally, all specimens exhibit a weld depth that is greater than their respective ledge thickness at the edge of ledge (the narrowest point). This indicates, for the given ledge thicknesses, all material at the edge of the ledge was consumed by the weld's

melt pool. Not only this, but additional material was deposited below the area that the ledge had previously occupied.

Following the analysis of this experimental data, a specimen was prepared implementing the conclusions drawn. The following chapter lays out the implementation of the iterative hybrid manufacturing method to prepare a two-walled specimen geometry presenting tool reach and access restrictions.

CHAPTER 4. IMPLEMENTATION OF ITERATIVE HM METHOD

The prescribed iterative hybrid manufacturing method was implemented to produce a sample with tall geometry presenting typical reach and access restrictions. This sample consists of two rectangular walls separated by a small distance (Figure 4.1). The component height of the two walls is H_c = 1.00” (25.40 mm). The two walls are separated by a distance D = 0.30” (7.62 mm).

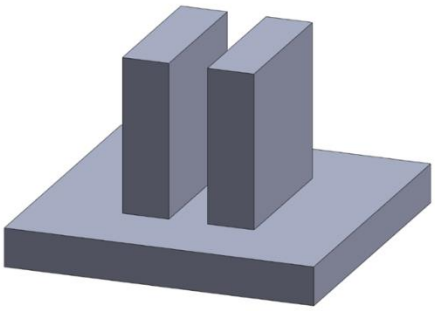

Figure 4.1 Implementation geometry

Machine tooling was selected to accommodate the requirements of the sample’s geometry. Three machine tools were utilized in the production of this sample component— 1) a 4-flute flat end mill of length T_ℓ = 0.50” (12.70 mm) and diameter d_1 = 0.50” (12.70 mm), 2) a 4-flute ball end mill of length T_ℓ = 0.50” (12.70 mm) and diameter d_1 = 0.25” (6.35 mm), and 3) a 4-flute lollipop end mill of length T_ℓ = 0.483” (12.26 mm) and cutting diameter d_1 = 0.25” (6.35 mm) with an included angle of θ = 300°, resulting in a shank diameter of d_2 = 0.125” (3.18 mm).

Utilizing the iterative hybrid manufacturing method, this tall geometry, i.e. the rectangular walls, was split into multiple slabs. A slab height of H_s = 0.30” (7.62 mm) and a slab allowance of A_s = 0.05” (1.27 mm) were set for the geometry. The resulting component section height was then H_R = 0.25” (6.35 mm) for a given cycle of deposition and subsequent machining. The component height, H_c = 1.00” (25.40 mm) was then broken into four (4) separate slabs. After these parameters had been identified, machine code was generated, and production of the sample geometry began. Table 4.1 provides a summary of the deposition parameters utilized in this implementation.

Table 4.1 Parametric description of deposition cycles

Process Variable	Set Level	
	Metric	Standard
laser power	*300 Watts*	
travel speed	*650 mm/min*	*25.59 in./min*
powder feed rate	*3.1 g/min*	*0.11 oz/min*
carrier gas flow	*4.0 L/min*	*0.14 CFM*

Process Variable	Set Level	
	Metric	Standard
shield gas flow	*8.0 L/min*	*0.28 CFM*
laser spot size	*1 mm*	*0.0394 in.*
standoff distance	*10 mm*	*0.3937 in.*
layer height	*0.1905 mm*	*0.0075 in.*
slab height	*7.62 mm*	*0.30 in.*

Machining throughout this implementation consisted of the two categories, face milling and profile milling, as identified in Section 3.1.1 above. The face milling operation was conducted to remove the slab allowance, while the profile milling was used to create the contour along the side of the component and the ledge for subsequent depositions. Based on the analysis of the data collected from the previous experiment, a ledge thickness of α = 0.01” (0.25 mm) was selected. As no apparent trend related to ledge thickness was identified, the value that would present the maximum material condition was selected to allow a greater deal of flexibility to the machining processes if issues arose. The same ledge overhang, β = 0.025” (0.64 mm), and ledge radius, R = 0.125” (3.18 mm), from the previous experiment were implemented.

Machining was segmented further into three steps, one for each of the machine tools used. The initial machining step, the face milling operation, utilized the flat end mill to remove the slab allowance. The second step was a precautionary ball end-milling cycle, running along the contour of the part to remove any excess and unanticipated material from the sides of the slab. The targeted material for this operation would exist outside the machining allowance and if not removed would increase the chip load of the next operation and present possible collision conditions. The final machining step was conducted utilizing

the lollipop end mill. To reduce the loading of the lollipop endmill, multiple passes at the initial z-height were taken and the tool was stepped up from the base of the component section. Three (3) passes were made at the initial z-height at depths of 0.010” (0.25 mm), 0.020” (0.51 mm), and 0.025” (0.64 mm) before the tool was stepped up in 0.01” (0.25 mm) intervals at a depth of 0.025” (0.64 mm).

Figure 4.2 depicts the first cycle of material deposition and machining. The first slab of material (Figure 4.1a) presented an overall height of approximately 0.30” (7.62 mm) in the center; however, the height at the edges of the part was insufficient, i.e. less than the required 0.25” (6.35 mm). This was identified via visual inspection after completing the face milling operation. The resulting top surface exhibited material deficiencies along the edges of the component. To correct for this, the slab allowance was increased from the initial A_s = 0.05” (1.27 mm) to A_s = 0.10” (2.54 mm). Figure 4.2b depicts the results of the face milling with the adjusted slab allowance. After this minor correction, no issues arose, and the machining cycle continued to

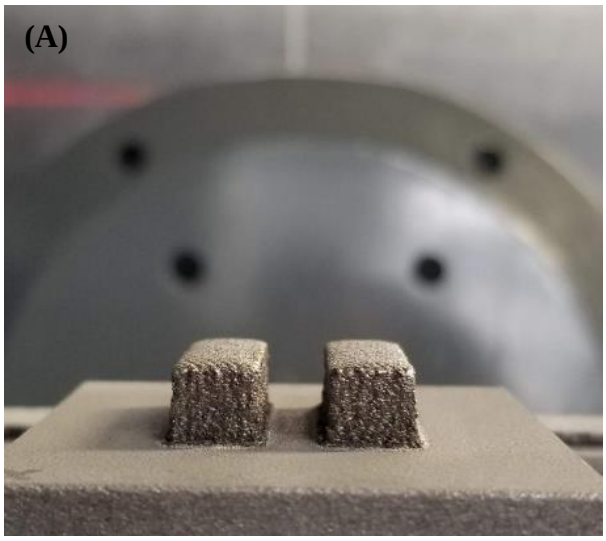

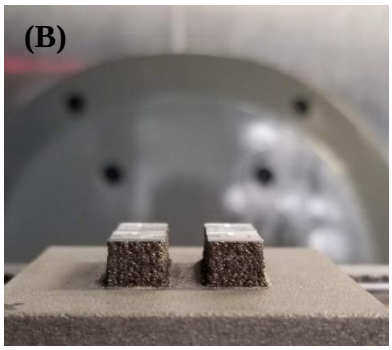

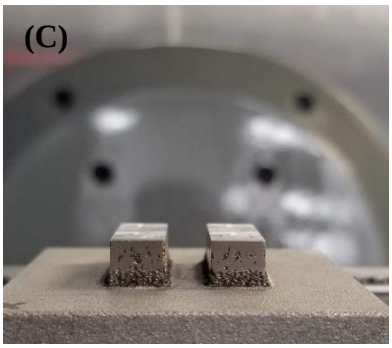

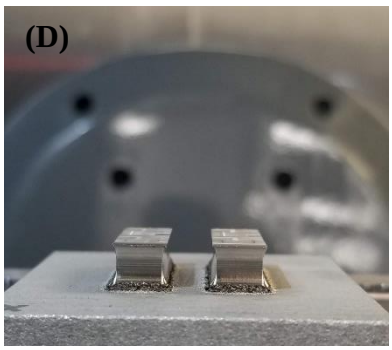

Figure 4.2 First deposition and machining cycle; (a) initial deposition, (b) results of face milling, (c) removal of excess material via ball end milling, (d) creation of ledge geometry

profile milling. Figure 4.2c depicts the results of the ball-milling operation which removed the material in excess of the machining allowance, while Figure 4.2d shows the component and ledge geometry after all machining was complete for the first cycle.

Following the successful completion of the first deposition and machining cycle, a second iteration was conducted (Figure 4.3). After offsetting the work coordinates of the machine by the resulting component height, the second cycle was conducted in the same manner as the initial cycle. In fact, the same machine code was able to be used for the deposition. An altered version was necessary for the machining cycles for two reasons: 1) the adjustment of the slab allowance for the face milling operation and 2) additional depth cuts (passes at different z-heights) were necessary to remove the remaining machining allowance and the ledge left on the initial cycle. To clarify, the profile milling of the initial deposition consisted of machining at five (5) depth cuts, while the second cycle consisted of nineteen (19) depth cuts.

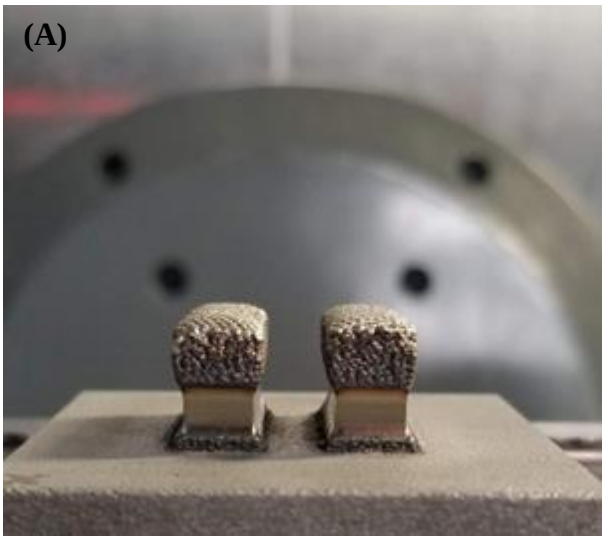

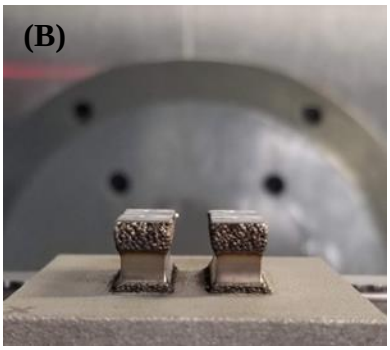

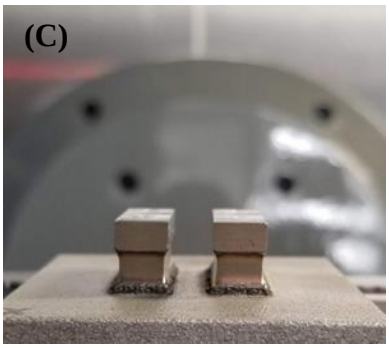

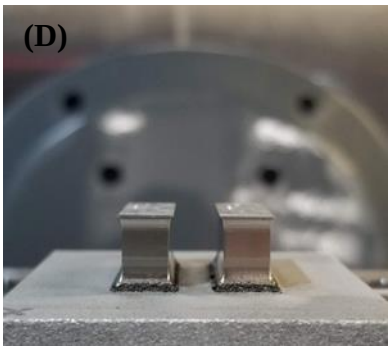

Figure 4.3 Second deposition and machining iteration; (a) deposition on existing component and ledge, (b) results of face milling, (c) removal of excess material via ball end milling, and (d) creation of ledge and component geometry at completion of second cycle

With no further adjustments necessary (except offsetting the work coordinates), a third and fourth iteration of the deposition and machining cycle were conducted (Figure 4.4). It should be noted that following the adjustment of the slab allowance, the resultant height of

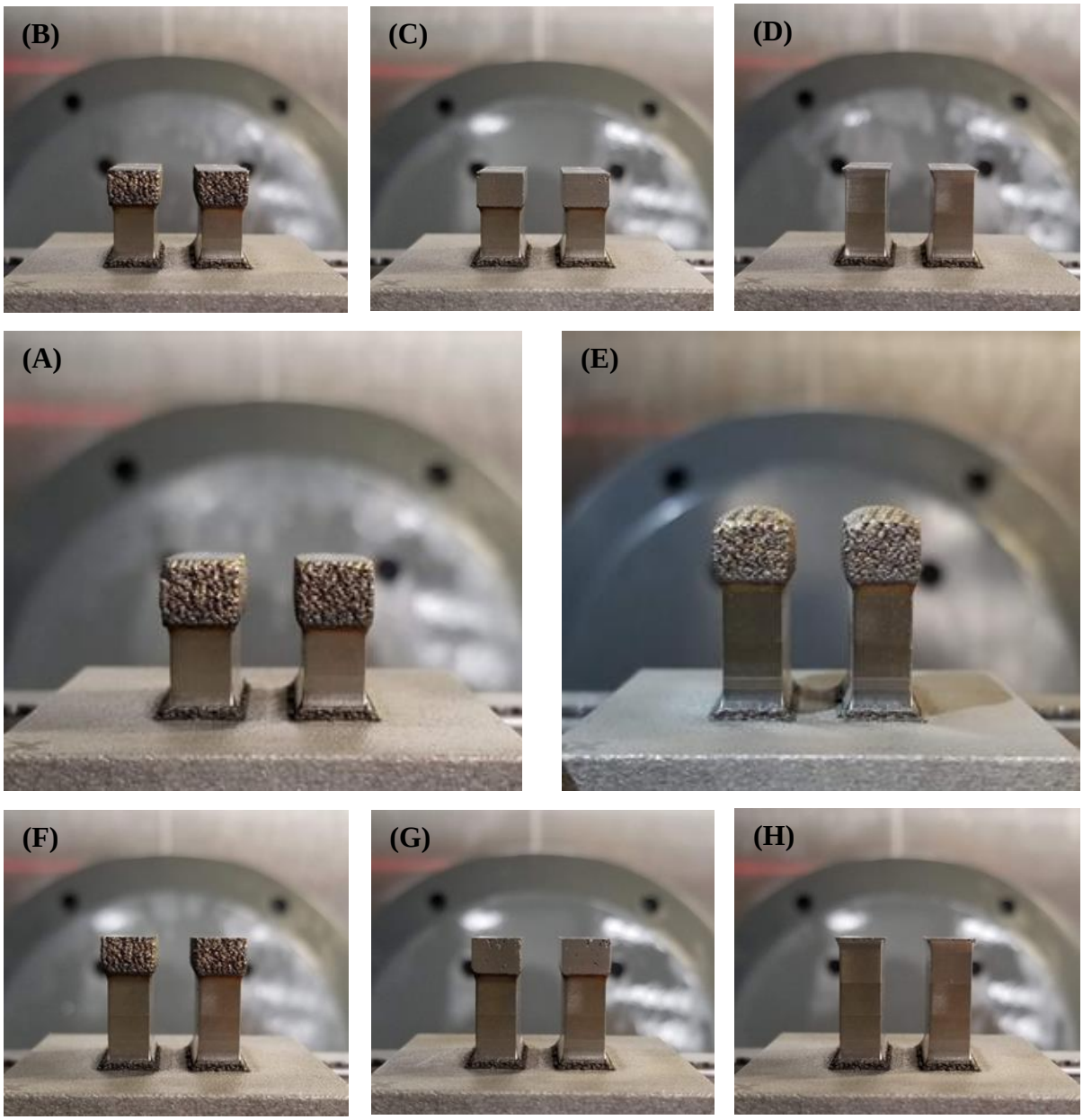

Figure 4.4 Third and fourth deposition and machining iterations;

Third iteration: (a) deposition on existing component and ledge, (b) results of face milling, (c) removal of excess material via ball end milling, and (d) creation of ledge geometry

Fourth iteration: (e) deposition on existing component and ledge, (f) results of face milling, (g) removal of excess material via ball end milling, and (h) creation of ledge geometry

the section was $H_R = 0.20$” (5.08 mm). Therefore, the fourth iteration did not achieve the final component height as initially intended. An additional slab and five (5) total iterations were necessary.

The fifth and final machining cycle consisted of the same deposition cycle as the previous four (4) iterations (Figure 4.5a) and a modified machining cycle. This modified machining cycle used the same face milling step as previous iterations (Figure 4.5b) but utilized the ball end mill to complete all profile milling rather than segmenting into two (2) steps. As the supporting ledge is no longer necessary, the component was simply machined to the final specifications (Figure 4.5c). With the completion of this final iteration, the final geometry was created, and the implementation complete.

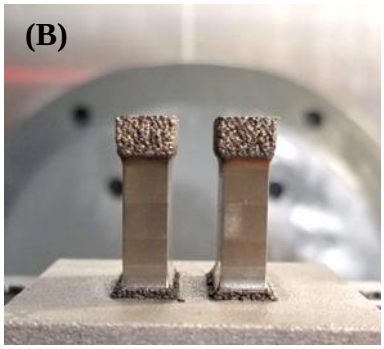

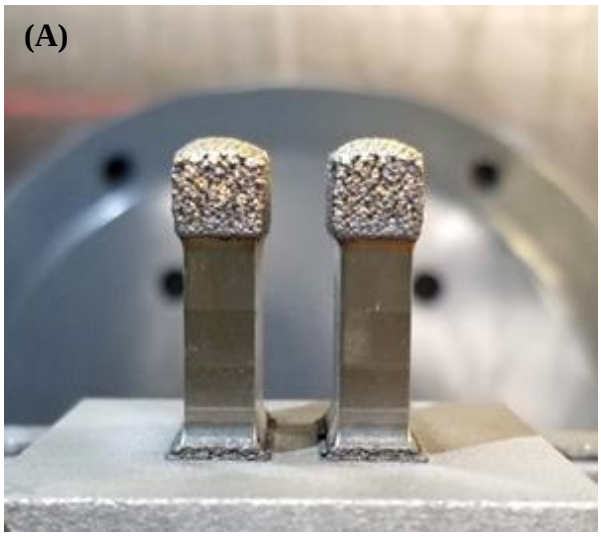

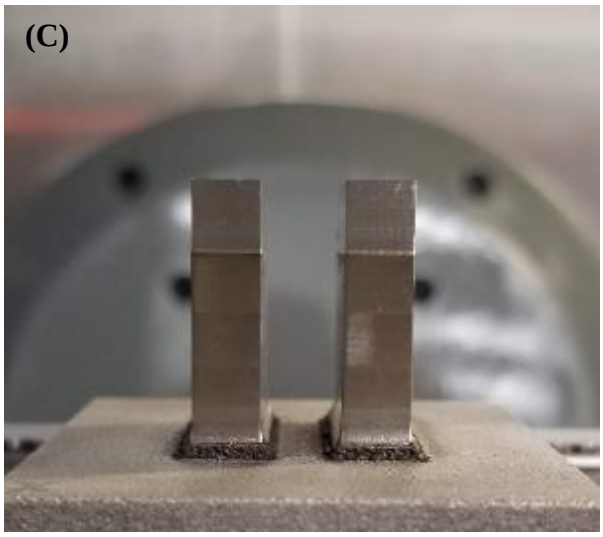

Figure 4.5 Final deposition and machining cycle; (a) deposition on existing component and ledge, (b) results of face milling, and (c) final component geometry

The implementation of the method was successful in effectively segmented the walls of the "tall" geometry into smaller slabs while still allowing future depositions to occur. This enabled the use of short machine tools. As shown in Figure 4.6, the reach of the machine tool used to machine the contour of the walls is significantly shorter than the walls themselves. The component height, H_c = 1.00" (25.40 mm), is greater than two times the reach of the lollipop end mill, T_ℓ = 0.483" (12.26 mm). The overall length of the machine tool, including the portion of the shank without a reduced diameter, is, however, approximately equivalent to the height of the components produced. The height of the geometry reached in this implementation is not the limit of this method; the height of this geometry, 1.00" (25.40 mm), is simply where the implementation was stopped. The component height can be increased to be more representative of the extreme or severe cases of tool reach requirements, and even beyond these traditional limits.

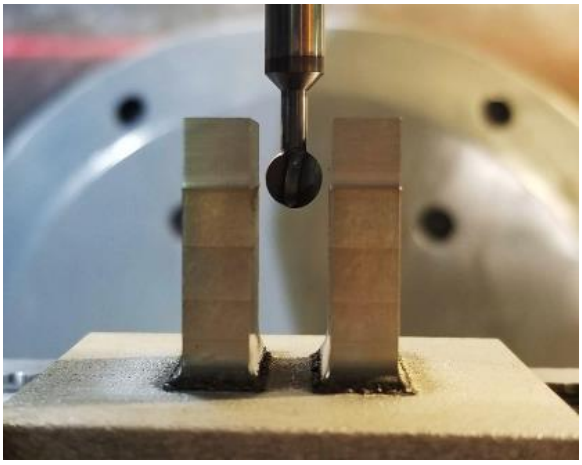

Figure 4.6 Comparison of final component to lollipop end mill

This implementation was not without error. As previously mentioned, the actual slab height was inaccurately predicted requiring an increase in the slab allowance. Additional error is apparent when looking at the machining marks that indicate where each slab's contour machining operations stopped. These marks are not equally separated, as expected for slabs 2 and 3. This is likely caused by human error in adjusting work coordinates between slabs. Additionally, in the case of the final slab, where ball milling was conducted along the contour, the machine tool was likely not brought down far enough leaving a small scallop.

CHAPTER 5. CONCLUSIONS AND FUTURE WORK

This thesis has presented a new process planning approach for iterative, in-envelope hybrid manufacturing (HM). An exploration of the process parameters for such an approach and their interaction with each other was conducted. This approach utilizes a novel support structure method— selectively removing the machining allowance on the contour of the part to leave a shelf or *ledge* of material. Parameters describing the geometry of this ledge were of particular interest and were investigated further, specifically the ledge thickness. Experiments were conducted using an HM system combining a laser-heated, blown-powder variant of directed energy deposition (laser metal deposition, LMD) with computer numerical control (CNC) machining.

5.1 Conclusions

Utilization of this novel process planning approach resulted in the successful creation of a sample with two "tall" walls that presented typical tool reach and access restrictions. By segmenting this sample into shorter *slabs*, these restrictions were effectively mitigated allowing the use of machine tools significantly shorter than the overall height of the part. This method proved successful in the use of 3-axis toolpaths for both material deposition and the removal of the machining allowance. Experiments with ledge thickness yielded no apparent trends between ledge thickness and deviation from expected component height or the resulting weld depths. However, the experiments did present weld depths at the edge of the machined ledge in excess of the selected ledge thickness values.

5.2 Future Work

Following the successful implementation of this method, significant areas for future research exists. Initial experimentation with the value of ledge thickness (α) was conducted;

this parameter could be explored further with larger values of α, different power settings for the laser, and even different AM processes. As demonstrated by the implementation in Chapter 4, the error in layer height is not yet fully understood; further research on the accumulation of this error and how it relates to a given layer height is possible. Research on the appropriate selection of slab allowance and other process parameters would also be beneficial in providing a more optimal process.

The targeted geometry for this thesis was tall, straight walls. Expansion to freeform geometries is desired, as such the spherical ball end was utilized as this will likely present the most attractive undercut tooling option. However, there exists potential to utilize additional undercut machine tools, such as t-slot and dovetail cutters, in combination with the lollipop endmill. To date, the heights of all slabs have been equal; this is not a requirement. Slab heights can be varied to accommodate these freeform geometries. Additionally, machining parameters to date are not necessarily optimal; future work is necessary to optimize machining parameters. The surface roughness of the implemented geometry was not tested. A comparison of the surface roughness of parts produced using the presented method and parts produced using long machine tools should be conducted.

The work in this thesis focused primarily on the geometric implications of the process parameters; the thermal implications of such a method need to be explored further. The metallurgical consequences of machining and then depositing again are still unclear. Geometric distortion of the existing slab geometry and the ultimate strength of the final part could be of concern. Further investigation into these properties is necessary for this method to be considered for production of functional components.

REFERENCES

[1] "3D Printing as Manufacturing," *Kuunda 3D Printing*, 08 February 2018. [Online]. Available: https://kuunda3d.com/3d-printing-as-manufacturing/. [Accessed 17 May 2019].

[2] I. Wright, "Hybrid Manufacturing & The Future of 3D Printing for Production," *engineering.com*, 24 September 2018. [Online]. Available: https://www.engineering.com/AdvancedManufacturing/ArticleID/17717/Hybrid-Manufacturing-The-Future-of-3D-Printing-for-Production.aspx. [Accessed 25 May 2019].

[3] J. Bennett *et al.*, "Repairing Automotive Dies With Directed Energy Deposition: Industrial Application and Life Cycle Analysis," *J. Manuf. Sci. Eng.*, vol. 141, no. 2, 2019.

[4] P. Zelinski, "Metal 3D Printing in a Machine Shop? Ask the Marines," *Additive Manufacturing Magazine*, 10 April 2019. [Online]. Available: https://www.additivemanufacturing.media/blog/post/metal-3d-printing-in-a-machine-shop-ask-the-marines. [Accessed 27 May 2019].

[5] S. Flank, A. R. Nassar, T. W. Simpson, N. Valentine, and E. Elburn, "Fast Authentication of Metal Additive Manufacturing," *3D Print. Addit. Manuf.*, vol. 4, no. 3, pp. 143–148, 2017.

[6] "Hybrid Manufacturing Resources," *Hybrid Manufacturing Technologies Ltd*, 2018. [Online]. Available: http://www.hybridmanutech.com/resources.html. [Accessed 27 May 2019].

[7] "Hybrid Metal Manufacturing: a core application for Optomec additive manufacturing solutions," *Optomec, Inc.*, 2018. [Online]. Available: https://www.optomec.com/3d-printed-metals/lens-core-applications/hybrid-manufacturing/. [Accessed 28 May 2019].

[8] T. W. Simpson, "What Is Directed Energy Deposition?," *Modern Machine Shop*, 25 January 2019. [Online]. Available: https://www.mmsonline.com/blog/post/what-is-directed-energy-deposition. [Accessed 27 May 2019].

[9] Q. Zeng, Z. Xu, Y. Tian, and Y. Qin, "Advancement in additive manufacturing & numerical modelling considerations of direct energy deposition process," in *Proceeding of the 14th International Conference on Manufacturing Research: Advances in Manufacturing Technology XXX*, 2016, pp. 104–109.

[10] K. A. Lorenz, J. B. Jones, D. I. Wimpenny, and M. R. Jackson, "A review of hybrid manufacturing," in *26th Solid Freeform Fabrication Symposium Conference Proceedings*, 2015, vol. 53, pp. 96–108.

[11] "Directed Energy Deposition," *Loughborough University*, 2019. [Online]. Available: https://www.lboro.ac.uk/research/amrg/about/the7categoriesofadditivemanufacturing/directedenergydeposition/. [Accessed 27 May 2019].

[12] S. W. Williams, F. Martina, A. C. Addison, J. Ding, G. Pardal, and P. Colegrove, "Wire+ arc additive manufacturing," *Mater. Sci. Technol.*, vol. 32, no. 7, pp. 641–647, 2016.

[13] J. B. Jones, "Image of nozzle." 31 October 2018.

[14] M. Rombouts, G. Maes, W. Hendrix, E. Delarbre, and F. Motmans, "Surface Finish after Laser Metal Deposition," *Phys. Procedia*, vol. 41, pp. 810–814, 2013.

[15] J. B. Jones, "The synergies of hybridizing CNC and additive manufacturing," *Hybrid Manuf. Technol. Ltd*, 2014.

[16] M. Hoefer, N. Chen, and M. Frank, "Automated Manufacturability Analysis for Conceptual Design in New Product Development," in *IIE Annual Conference. Proceedings*, 2017, pp. 860–865.

[17] "Air Cooled Yamaha Engine Block For Motorcycle , Wear Resistant DF 125cc," *China Good Quality Motorcycle Cylinder Supplier*, 2019. [Online]. Available: http://www.motorcycle-cylinder.com/sale-9697493-air-cooled-yamaha-engine-block-for-motorcycle-wear-resistant-df-125cc.html. [Accessed 28 May 2019].

[18] D. L. Bourell, J. J. Beaman Jr, D. Klosterman, I. Gibson, and A. Bandyopadhyay, "Rapid Prototyping," *ASM Handb.*, vol. 21, pp. 383–387, 2001.

[19] R. C. Sanders Jr, J. L. Forsyth, and K. F. Philbrook, "3-D model making." Google Patents, 1998.

[20] "Solidscape 3D printers," *Solidscape, Inc.*, 2018. [Online]. Available: https://www.solidscape.com/products/3d-printers/. [Accessed 17 November 2019].

[21] R. Merz, F. B. Prinz, K. Ramaswami, M. Terk, and L. E. Weiss, "Shape deposition manufacturing," in *1994 International Solid Freeform Fabrication Symposium*, 1994.

[22] Matsuura Machinery USA, "LUMEX Series." [Online]. Available: http://matsuurausa.com/series/lumex-series/. [Accessed 28 May 2019].

[23] A. Hussein, L. Hao, C. Yan, R. Everson, and P. Young, "Advanced lattice support structures for metal additive manufacturing," *J. Mater. Process. Technol.*, vol. 213, no. 7, pp. 1019–1026, 2013.

[24] Mazak Corporation, "INTEGREX i-400AM," 2019. [Online]. Available: https://www.mazakusa.com/machines/integrex-i-400am/. [Accessed 30 June 2019].

[25] T. Yamazaki, “Development of A Hybrid Multi-tasking Machine Tool: Integration of Additive Manufacturing Technology with CNC Machining,” *Procedia CIRP*, vol. 42, pp. 81–86, 2016.

[26] I. Optomec, “3D Printed Metals - LENS Metal Additive Manufacturing Technology,” 2018. [Online]. Available: https://www.optomec.com/3d-printed-metals/lens-technology/. [Accessed 30 June 2019].

[27] DMG MORI, “Powder Nozzle - ADDITIVE MANUFACTURING machines from DMG MORI,” 2019. [Online]. Available: https://us.dmgmori.com/products/machines/additive-manufacturing/powder-nozzle. [Accessed 30 June 2019].

[28] R. Dwivedi and R. Kovacevic, “Process planning for multi-directional laser-based direct metal deposition,” *Proc. Inst. Mech. Eng. Part C J. Mech. Eng. Sci.*, vol. 219, no. 7, pp. 695–707, 2005.

[29] L. Ren, T. Sparks, J. Ruan, and F. Liou, “Process planning strategies for solid freeform fabrication of metal parts,” *J. Manuf. Syst.*, vol. 27, no. 4, pp. 158–165, 2008.

[30] L. Ren, T. Sparks, J. Ruan, and F. W. Liou, “Integrated process planning for a multiaxis hybrid manufacturing system,” *J. Manuf. Sci. Eng.*, vol. 132, no. 2, April 2010.

[31] A. B. Varotsis, “How to design parts for CNC machining,” *3D Hubs*, 2019. [Online]. Available: https://www.3dhubs.com/knowledge-base/how-design-parts-cnc-machining. [Accessed 25 May 2019].

[32] Harvey Performance Company, “Multi-Functional Tools Every Shop Should Have,” *In The Loupe*, 23 March 2018. [Online]. Available: https://www.harveyperformance.com/in-the-loupe/multi-functional-tools/. [Accessed 20 October 2019].